Hereditary myopathy with early respiratory failure associated with a mutation in A-band titin

Ohlsson, Monica; Hedberg, Carola; Brådvik, Björn; Lindberg, Christopher; Tajsharghi, Homa; Danielsson, Olof; Melberg, Atle; Udd, Bjarne; Martinsson, Tommy; Oldfors, Anders

Published in:
Brain

DOI:
10.1093/brain/aws103

2012

Hereditary myopathy with early respiratory failure associated with a mutation in A-band titin

M. Ohlsson,[1*] C. Hedberg,[1*] B. Brådvik,[2] C. Lindberg,[3] H. Tajsharghi,[1] O. Danielsson,[4] A. Melberg,[5] B. Udd,[6,7,8] T. Martinsson[9] and A. Oldfors[1]

1 Department of Pathology, University of Gothenburg, Sahlgrenska University Hospital, SE-413 45 Gothenburg, Sweden

2 Department of Clinical Sciences, Division of Neurology, Lund University, SE-221 85 Lund, Sweden

3 Department of Neurology, University of Gothenburg, Sahlgrenska University Hospital, SE-413 45 Gothenburg, Sweden

4 Neuromuscular Unit, Department of Neurology, Linkoping University, SE-581 85 Linkoping, Sweden

5 Department of Neuroscience, Neurology, Uppsala University, Uppsala University Hospital, SE-75185 Uppsala, Sweden

6 Neuromuscular Center, Tampere University and Hospital, 33520 Tampere, Finland

7 Department of Neurology, Vasa Central Hospital, 65130 Vasa, Finland

8 Folkhälsan Genetic Institute, Department of Medical Genetics, Helsinki University, 00014 Helsinki, Finland

9 Department of Clinical Genetics, University of Gothenburg, Sahlgrenska University Hospital, SE-413 45 Gothenburg, Sweden

* These authors contributed equally to this work

Correspondence to:
Anders Oldfors MD, PhD
Department of Pathology
Institute of Biomedicine
University of Gothenburg
Sahlgrenska University Hospital
SE-413 45 Gothenburg
Sweden

anders.oldfors@gu.se

Short running title: Titin A-band mutation in myopathy with respiratory failure

Abstract

Hereditary myopathy with early respiratory failure and extensive myofibrillar lesions have been described in sporadic and familial cases and linked to various chromosomal regions. The mutated gene is unknown in most cases.

We studied eight individuals from three apparently unrelated families with clinical and pathological features of hereditary myopathy with early respiratory failure. The investigations included clinical examination, muscle histopathology and genetic analysis by whole exome sequencing and single nucleotide polymorphism arrays.

All patients had adult onset muscle weakness in the pelvic girdle, neck flexors, respiratory and trunk muscles, and the majority had prominent calf hypertrophy. Examination of pulmonary function showed decreased vital capacity. No signs of cardiac muscle involvement were found.

Muscle histopathological features included marked muscle fibre size variation, fibre splitting, numerous internal nuclei and fatty infiltration. Frequent groups of fibres showed eosinophilic inclusions and deposits. At the ultrastructural level there were extensive myofibrillar lesions with marked Z-disc alterations.

Whole exome sequencing in four individuals from one family revealed a missense mutation, g.274375,T>C; p.Cys30071Arg, in the titin gene, *TTN*. The mutation, which changes a highly conserved residue in the myosin binding A-band titin, was demonstrated to segregate with the disease in all three families. High density single nucleotide polymorphism arrays covering the entire genome demonstrated sharing of a 6,99 Mb haplotype, located in chromosome region 2q31 including *TTN*, indicating common ancestry.

Our results demonstrate a novel and the first disease-causing mutation in A-band titin associated with hereditary myopathy with early respiratory failure. The typical histopathological features with prominent myofibrillar lesions and inclusions in muscle and respiratory failure early in the clinical course should be incentives for analysis of *TTN* mutations.

Key words:

Myopathy; respiratory failure; exome sequencing; titin; mutation

Abbreviations:

HMERF: hereditary myopathy with early respiratory failure
SNP: Single nucleotide polymorphism

Introduction

Respiratory failure as an early symptom in ambulant patients with inherited primary muscle diseases is uncommon. However, early respiratory failure is a frequent complication in a group of myopathies with characteristic myofibrillar lesions and cytoplasmic bodies (Jerusalem *et al.*, 1979; Patel *et al.*, 1983; Winter *et al.*, 1986; Chapon *et al.*, 1989; Edström *et al.*, 1990; Chinnery *et al.*, 2001; Tasca *et al.*, 2010). These myopathies have more recently been referred to as hereditary myopathy with early respiratory failure (HMERF; OMIM#603689). Previous studies have indicated that they are genetically heterogenous. The family described by Chapon *et al*. (Chapon *et al.*, 1989) demonstrated linkage to 2q21 (Xiang *et al.*, 1999) whereas two of the families that Edström et al described were linked to 2q31 (Nicolao *et al.*, 1999). Sequence analyses in these two families demonstrated a heterozygous mutation (R279W) in the protein kinase domain of titin (*TTN*) (Lange *et al.*, 2005). No other causative mutations have been demonstrated.

We describe the clinical, histopathological and muscle magnetic resonance imaging findings in eight individuals from three apparently unrelated Swedish families, with a dominantly inherited adult-onset myopathy characterized by proximal and distal muscle weakness and early respiratory failure compatible with a diagnosis of HMERF. Muscle histopathological features included extensive myofibrillar changes, fibre size variability, prominent fibre splitting, increased internal nuclei, rimmed vacuoles and frequent eosinophilic inclusions. Genetic analysis in our patients by whole exome sequencing disclosed a missense mutation in the C-terminal part of myosin binding A-band titin that was the apparent cause of disease in these families. This was further supported by a unique common haplotype using high-density single nucleotide polymorphism (SNP) arrays covering the entire genome.

Materials and methods

Patients and muscle biopsy

The study was approved of by the Regional Ethics Committee. Eight patients were examined clinically, six patients from family A, one patient from family B and one patient from family C (Fig. 1). Clinical data of deceased patients were obtained from case records and relatives. Muscle weakness was evaluated according to the Medical Research Council scale (MRC). Investigations of the patients included serum levels of creatine kinase, 12-lead electrocardiogram, echocardiogram and pulmonary function tests. Electromyography was performed in three patients. Magnetic resonance imaging was performed in two patients from family A (patient III:14 and IV:6) of pelvic and lower limb on a 1,5T MR scanner.

Muscle biopsy was performed in seven of the affected patients, and in four of these a second biopsy was obtained after seven to ten years. Specimens were frozen in propane chilled by liquid nitrogen for histochemical analysis and fixed in glutaraldehyde for electron microscopy. Standard techniques were applied for histochemical staining of cryostat sections and for electron microscopy. Immunohistochemical analysis was performed with antibodies against NCAM (CD56; Becton Dickinson), desmin (Dako), dystrophin (Novocastra), titin (Biocytex), alpha-B-crystalline (Novocastra), and myotilin (Novocastra). EnVision Flex (Dako) was used to visualize immunoreactive material. Analysis of actin was performed by incubation of sections with phalloidin-rhodamine and fluorescence microscopy.

Genetic analysis

Exome sequencing

Genomic DNA extracted from blood samples from two affected (III:14 and III:16) and two healthy (IV:2 and IV:5) members of family A were analyzed. Enrichment of coding exons and flanking intronic regions totaling 50Mb was performed with the SureSelect human all exon kit

following the manufacturer's standard protocol (Agilent). The DNA library consisting of paired-end reads was sequenced on an Illumina HiSeq 2000 instrument following the manufacturer's standard protocol (Illumina, SanDiego, CA, USA).

Base calling was performed by the Illumina pipeline with default parameters. All the raw reads were aligned to the reference human genome (UCSChg19) using the Burrows-Wheeler alignment (BWA) (Li and Durbin, 2009). SNPs and indels were identified using the Genome Analysis Tool Kit (GATK) (DePristo *et al.*, 2011). SNPs and indels with a Phred-like variant quality score of at least 30 were filtered against dbSNP131 and the 1000 Genome project to exclude previously identified SNPs. Novel insertions/deletions, splice-site, missense and nonsense variants were excluded if detected in any of the two healthy individuals. Filtering against other in-house sequenced exomes was then performed to further reduce the number of candidate mutations. Functional consequences of the remaining non-synonymous variants were predicted using the SIFT algorithm and information regarding conservation for the variants among vertebrate species (phyloP score) by applying the UCSC genome browser. Variants that were predicted to be tolerated and/or not conserved among vertebrates were excluded.

Sanger sequencing

Sanger sequencing was performed using standard techniques of PCR amplicons with primers from genomic DNA to confirm the presence and identity of the variants in the *ABCB11* and *TTN* gene after they had been identified by exome sequencing (primer sequences are available on request).

Array analysis

SNP array analysis was performed as previously described (Caren *et al.*, 2008). Affymetrix 250K SNP arrays (Affymetrix, Santa Clara, CA) were used and data analysis was performed using GDAS (GeneChip® DNA Analysis software) and GTYPE (Affymetrix) for extraction

of genotype calls.

SNP genotype data for the individuals were analyzed to identify regions free from incompatibilities. Data for six affected family members of pedigree A (III:14, III:16, IV:1, IV:4, IV:6 and IV:7), one in pedigree B (II:1) and one in pedigree C (II:1) were analyzed to identify genomic regions fitting an autosomal dominant genetic model. The method is indirect in that it scores loci where the dominant gene cannot be localized, with the aim of finding a region where no such incompatibilities occur, *i.e.* the inferred disease locus. For each SNP locus individuals can have either genotype calls "AA", "AB", "BB" or a "NoCall". A locus where at least one affected individual is "AA" and at least one other affected individual is "BB", is scored as an incompatibility. Such a locus is therefore an "incompatibility" and can by definition not be included in the correct disease gene haplotype. In contrast, a continuous region of SNP loci, without any incompatibilities among affected individuals, may include a unique disease haplotype and consequently also the disease gene. Genotypes for all analyzed affected individuals were compared and incompatibilities as defined above for all the approximately 260.000 SNP loci were scored and plotted against the genome position for each locus. Corresponding genotype data generated by Affymetrix 250k array for 25 healthy control individuals corresponding to 50 haplotypes were included in the analyses. All genomic positions for SNPs are given relative to the Feb. 2009 – GRCh37/hg19 genome assembly.

Results

Clinical features

Family A

All patients had a normal perinatal period and motor development. Six patients were clinically investigated (Table 1). Age at onset of disease in these patients varied from 18 to 40 years.

The muscle weakness was slowly progressive and symmetrically distributed. Muscle atrophy was not a prominent finding. In two patients, myalgia was an early symptom. Muscle weakness in the pelvic girdle was found in all patients and in three patients, muscle weakness was also found in the shoulder girdle. There was no winging of scapula. The neck flexors and trunk muscles were severely affected in all patients and they had a prominent calf hypertrophy. Knee flexor and ankle dorsiflexor muscle weakness was seen in five patients. All patients were ambulatory but showed signs of respiratory insufficiency with decreased vital capacity (range 20 to 74 % of predicted value) (Table 2). Three patients needed a ventilator at night, from age 35, 37 and 55 years. Serum creatine kinase was either normal or slightly elevated (analyzed in three patients). Electromyography was performed in one patient and showed myopathic changes. Electrocardiography and echocardiography were performed in all six patients and no signs of cardiomyopathy were found.

Family B

The two affected patients from family B had a normal birth and neonatal period. The motor development was normal. Patient B I:1 died by respiratory failure at age 51. Patient B II:1 first noticed muscle weakness in the ankle dorsiflexors with frequent falls at age 22 and mild muscle atrophy was noticed after a few years. Clinical examination at age 30 years showed moderate to severe weakness in both pelvic and shoulder girdle muscles (MRC grade 2-3). There was no scapular winging. The neck flexor, trunk and ankle dorsiflexor muscles were more severely affected (MRC grade 1-2). Weakness was also seen in the elbow extensor and flexor muscles (MRC grade 4) as well as in finger extensor and flexor muscles (MRC grade 2-3). There was prominent calf hypertrophy. At age 30 he was able to walk up to 5 kilometers but shortness of breath and myalgia were frequent symptoms. Electromyography showed myopathic changes. Electrocardiography and echocardiography showed no signs of cardiomyopathy.

The muscle weakness has been markedly progressive and from age 36 he had lost ambulation and needed a wheelchair. He had respiratory muscle weakness with shortness of breath from age 30 and needed a ventilator at night from age 39. Clinical examination at age 43 showed severe loss of function in most of the muscles in the lower extremities (Table 1) and severe muscle weakness in most of the muscles in the upper extremities. Blood PCO_2 was 8.1 kPa (normal value 4.4-6 kPa).

Family C

The two affected patients from family C had normal motor development. Patient C I:2, a male patient, died from respiratory insufficiency at age 73. He suffered from a myopathy, which was diagnosed at age 55 but was never further classified. In his daughter, patient C II:1, transient respiratory insufficiency was for the first time observed at age 36 when her youngest child was born. At about age 40 she began to notice proximal muscular weakness in her upper and lower extremities. There was also weakness in her foot extensors but not in her hands. Because of gradual progress of the muscular weakness the patient was referred for neurological examination at age 45. It demonstrated generalized muscular atrophy with corresponding weakness but sparing the facial muscles (Table 1). There was no winging of scapula. Cardiac examination by electrocardiography and ultrasound was normal. Electromyography showed generalized myopathy in all extremities, most pronounced in the proximal muscles. Pulmonary function test showed decreased vital capacity to 70% of the expected normal value.

Magnetic resonance imaging

Magnetic resonance imaging was performed in two patients in family A (Patient III:14 and IV:6). On T1-weighted sequences the fatty degenerative changes were symmetric and showed a unique distribution. In the pelvic region severe replacement was present in the iliopsoas, rectus abdominis, obturatorius, gluteus minimus and the proximal parts of the gluteus

maximus muscles. In the thighs there was an unusual gradient with proximal parts being more replaced than distal parts of the individual muscles. The vastus lateralis, intermedius and medialis, as well as the sartorius, gracilis and semitendinosus muscles were severely involved, whereas the adductor longus muscles were relatively spared (Fig. 2). All distal parts of the thighs showed only mild fatty infiltration. In the lower legs the anterior and lateral compartment muscles were severely affected, but there was notably less involvement of the long toe extensors in the younger patient (IV:6). In the posterior calves, the soleus and popliteus muscles showed moderate fatty replacement, whereas both the lateral and medial gastrocnemius muscles were spared. On fat suppression sequences no significant signal increase was observed.

Muscle pathology

There was marked fibre size variability with atrophic and hypertrophic fibres in all biopsy specimens. Many fibres showed numerous internally located nuclei and there were focal areas with frequent split fibres (Fig. 3). The characteristic pathological changes were focal, frequently with groups of several fibres showing marked alterations, whereas other regions were less affected or even normal. There was also great variation between different muscle biopsy samples with regard to degree of pathological changes. Some of the biopsy specimens revealed marked fatty infiltration. No association between fibre type and histopathological changes was found. Eosinophilic inclusions or deposits were seen in all samples. The deposits were red or dark green in trichrome stained sections and some of them had the appearance of cytoplasmic bodies (Fig. 3). The cytoplasmic body-like inclusions stained positive for F-actin using phalloidin-rhodamine fluorescence analysis (Fig. 4). Rimmed vacuoles were seen in all patients to some degree. Interstitial inflammatory cells were rare and seen in only one biopsy specimen. In NADH-tetrazolium reductase stained sections, fibres with unstained, "rubbed-out" regions were seen in more than half of the biopsies. No ragged red fibres were identified.

In two patients repeat biopsy was performed in the same muscle (tibialis anterior) (Table 3, patients A IV:4 and A IV:6). In both patients, the second biopsy showed advanced atrophy with fat tissue replacement.

Immunohistochemical analysis revealed N-CAM up-regulation in the majority of the muscle fibres (Fig. 5A). In several affected fibres with structural abnormalities there were accumulation of desmin, dystrophin and titin (Fig. 5B). There was also variable accumulation of myotilin and alpha-B crystalline.

By electron microscopy, Z-disk alterations were very frequent with Z-disk streaming and regions with extensive dispersion of semi-dense Z-disk material over the entire sarcomere (Fig. 6 and 7). There were also large regions with myofibrillar disruption and irregular electron-dense deposits (Fig. 6 and 7). Most of these deposits did not show the typical structure of cytoplasmic bodies but occasional cytoplasmic bodies surrounded by a halo of radially arranged thin filaments were found. Accumulation of granulo-filamentous material or dappled dense bodies as can be seen in desminopathy and some other myofibrillar myopathies were not identified. Structural alterations corresponding to rimmed vacuoles showed degradation products and lamellate myeloid structures. Collections of 15-20 nm tubulo-filaments were observed in one patient. Most mitochondria were structurally normal but a few contained paracrystalline inclusions.

Genetic analysis

Exome sequencing

Exome sequencing was performed in two healthy (IV:2 and IV:5) and two affected (III:14 and III:16) individuals of family A. Overall, approximately 43.4 million sequencing reads were produced for each of the samples and approximately 99% of these were aligned to the human reference genome (hg19) and 64% of these fell onto targeted and enriched exons (Table 4).

The exome coverage distribution showed that 80% of the exome had a read depth of 8x and

50% of the exome had a read depth of 30x. In each individual, between 38300 and 40200 variants were detected. In each individual, 4500 to 5040 variants (SNPs and indels) were not present in dbSNP131 or the 1000 Genome project, and of these 2386 to 2508 were nonsense, missense, framshift or splice site variants (Table 5). After exclusion of variants found in healthy individuals, 147 SNPs and 21 indels remained (Table 5). By further filtering of these against data from other in-house sequenced exomes and detection of possible pathogenic SNPs using SIFT algorithms, only four variants remained.

Two of these four variants were found in the gene *ZNF594* (Homo sapiens zinc finger protein 594, NM_032530) located on chromosome 17. These two missense variants were located in a non-conserved region and therefore unlikely to be causative of the disease. The third variant was in exon 18 of the *ABCB11* gene (ATP-binding cassette sub-family B member 11; NM_003742). It was a heterozygous mutation c.2093G>A, p.Arg698His, affecting a residue which is conserved among vertebrates but was recently reported in dbSNP134 as a polymorphism (rs138642043). The fourth variant was a heterozygous mutation g.274375T>C (AJ277892) in exon 343 of the *TTN* gene (Bang *et al.*, 2001), resulting in a novel, missense mutation p.Cys30071Arg (Q8WZ42), changing a residue which is highly conserved among vertebrates (Fig 8 and Supplementary material Fig 2). This was the obvious best candidate as a disease-causative mutation in familiy A.

Sanger sequencing

Sanger sequencing to study the identified *TTN* and *ABCB11* gene variants demonstrated that only the heterozygous *TTN* g.274375T>C mutation co-segregated with the disease in all three families. The mutation was not identified in any of 400 control chromosomes using Sanger sequencing.

Array analysis

DNA from selected members of the kindreds (Patients A III:14, A III:16, A IV:1, A IV:4, A

IV:6, A IV:7, B II:1 and C II:1) were subjected to analysis with Affymetrix 250k (260.000 SNPs) SNP arrays and subsequent data analyses. Analysis of the SNP array genotype data disclosed a region free of incompatibilities in chromosome region 2q (Fig. 9). In this region that spanned 7690 SNP loci there were very few incompatibilities – likely to be only rare genotyping errors. No other region in the genome came close in length to that on 2q. The region covers 6,99 Mb of DNA on chromosome region 2q, from marker rs6708551 in position 177,367,950 to marker rs2196690 in position 184,353,132 (Fig. 10 and Supplementary material Fig 1). Healthy control individuals (n=25) were analyzed (one at a time) together with the set of affected individuals. For all of these individuals the region on chromosome region 2q became covered with incompatibilities when they were analyzed one by one, indicating that the haplotype shared by the affected were not present in any of the 25 control individuals (50 possible healthy haplotypes). The shared haplotype was neither present in one of the individuals previously demonstrated with the mutation, R279W, in the protein kinase region of *TTN* reported by Lange *et al*. (Lange *et al.*, 2005). The data strongly indicate that the depicted region represents a disease containing shared haplotype among the affected members of family A, B and C.

Discussion

We describe eight individuals from three Swedish families with an adult-onset autosomal dominant myopathy demonstrating characteristic myofibrillar lesions. Respiratory insufficiency, with shortness of breath during exercise and decreased vital capacity, was present early in the clinical course and most patients needing ventilatory support at night were ambulatory.

The clinical and morphological characteristics are compatible with so-called hereditary myopathy with early respiratory failure (HMERF) (Edström *et al.*, 1990; Lange *et al.*, 2005). By whole exome sequencing we identified the apparent causative mutation in the titin gene,

TTN. Several lines of evidence support this conclusion. First, this was the best candidate mutation remaining after our filtering of all identified variants. Second, the mutation segregated with all affected individuals in the families. Third, the mutation is located in the gene encoding the giant muscle protein titin, containing 363 exons, which was already shown to be mutated in other HMERF patients just 15 exons from the present mutation (Lange *et al.*, 2005). Fourth, the mutation changes the highly conserved, small, uncharged and hydrophobic cysteine in position 30071 to the large, positively charged arginine. Fifth, it was not found in any of 400 control chromosomes. Sixth, genetic analysis in our three families with array data using SNP markers demonstrated that the affected individuals shared only one large haplotype on chromosome 2q31 corresponding to a 6,99 Mb region. This region encompasses 19 known genes including the titin gene (*TTN*).

Titin is more than one µm long and spans half the sarcomere, from the Z disk to the M line. It is known to contribute to the myofibril assembly providing specific attachment sites for different sarcomeric proteins and it has an important role in the mechanism of muscle elasticity (Labeit and Kolmerer, 1995; Krüger and Linke, 2011). The mutated residue in our three families is located in a myosin-binding fibronectin-III (FnIII) domain of A-band titin (A150) (Bucher *et al.*, 2010). The previously described HMERF mutation, R279W, in the close but more C-terminal kinase domain of titin was considered to act by disrupting the mechanosensor signaling complex associated with the mutated regulatory tail of the kinase. (Lange *et al.*, 2005). We excluded a mutation in the protein kinase domain in our patients by the exome sequencing as well as by Sanger sequencing. Our findings of a mutation in a relatively close but functionally completely different FnIII domain of the protein, causing an identical phenotype raise questions concerning the downstream molecular pathogenesis. Perturbed interaction with other sarcomeric proteins and possibly misfolding of defective titin protein may be common important factors leading to the same clinical and pathological

phenotype. The variable penetrance and diversity among affected individuals may be explained by a variable expression of the mutated allele and variations in the structure and composition of proteins interacting with titin.

The histopathological hallmark in our patients included eosinophilic inclusions or deposits that were red or dark green in trichrome staining. As in the original description of the patients, later demonstrated to carry a mutation in the kinase domain of titin, the inclusions were stained intensely with rhodamine conjugated phalloidin, which is a specific marker for F-actin (Edström *et al.*, 1990). Thus different *TTN* mutations cause similar pathological changes. By electron microscopy, irregular electrondense deposits were found, but they only rarely had the typical structure of cytoplasmic bodies with a halo of radially arranged thin filaments around the deposits. There were very frequent Z-disk alterations with Z-disk streaming and regions with extensive dispersion of semi-dense Z-disk material over the entire sarcomere and large regions with myofibrillar disruption. In addition there was muscle fibre necrosis and progressive replacement of muscle tissue by fibrous connective and fat tissue. Many of these features are typically found in myofibrillar myopathies (Selcen, 2011) and therefore, in terms of histopathological classification, HMERF should be considered to belong to this group of pathologically defined myopathies. An interesting finding was the variable degree of pathological changes in different parts of the same muscle biopsy. This is possibly due to variable expression of the mutated allele in different cells.

MRI examinations demonstrated selective involvement of specific muscles. In the pelvic region our patients showed fatty replacement mainly of the iliopsoas, rectus abdominis, obturatorius and gluteus minimus muscles. Severely affected muscles in the thighs were the semitendinosus, gracilis, sartorius muscles and the vastus lateralis, intermedius and medialis muscles, whereas the adductor longus muscles were relatively spared. In the lower legs there was fatty replacement predominantly in the anterior and lateral compartments. Muscle MRI

findings (Birchall *et al.*, 2005) in the family described by Chinnery *et al*. (Chinnery *et al.*, 2001) together with another British family and showed a similar pattern of involvement. and in one patient described by Tasca *et al*. (Tasca *et al.*, 2010) showed a very similar pattern of muscle involvement in different families suggesting that they may share a common pathogenetic mechanism.

Compared to the previously reported skeletal muscle titinopathies, HMERF is very dissimilar. The only other autosomal dominant disease is Tibial muscular dystrophy (TMD), a late onset distal myopathy without clinical involvement of respiratory functions or muscles in the upper limb/body regions (Udd *et al.*, 1993). This is caused by missense or nonsense mutations in the last two exons (362 and 363) of titin and the only similarity with HMERF is rimmed vacuolar pathology and involvement of anterior lower leg muscles. In homozygous state TMD mutations cause a very different early onset severe recessive LGMD2J (Udd *et al.*, 2005). Recessive nonsense mutations in the exons 358 and 360 are known to cause severe lethal cardiomyopathy with generalized skeletal myopathy with no clinical or pathological similarity to HMERF (Carmignac *et al.*, 2007).

The affected individuals shared a haplotype on chromosome 2q31 corresponding to a 6,99 Mb region indicating a common ancestry and a founder mutation in these apparently unrelated three families. Since the penetrance is variable and some individuals do not experience any symptoms until at high age, it is possible that many other familial and apparently sporadic cases share this mutation.

In conclusion we have identified three different Swedish HMERF families with a new mutation in the A-band titin. Further studies will show if this mutation and other *TTN* mutations cause most or all cases of HMERF.

Funding

The study was supported by a grant from the Swedish Research Council (Proj No 07122 to

AO), from the Selander Foundation (AM) and from the Sigrid Juselius Foundation and Folkhälsan Research Funds (BU).

Acknowledgements

The authors thank Dr Mats Geijer for assistance in reviewing the MRI examinations, Lili Seifi and Monica Jacobsson for skilled technical assistance and Staffan Nilsson for valuable comments on the haplotype analysis. Enrichment of coding exons and sequencing was performed at GATC Biotech AG (Konstanz, Germany).

Figures

Figure 1

Pedigree of family A, B and C. Black solid symbols = definitely affected, proven by characteristic muscle biopsy findings. Grey solid symbol = probably affected; clinical signs and symptoms of hereditary myopathy with early respiratory failure.

Figure 2

Axial T1-weighted lower limb magnetic resonance imaging of patient III:14 in family A shows severe degenerative change with fatty replacement at the pelvic level (A and B) in the iliopsoas, rectus abdominis, obturatorius, gluteus minimus and the proximal parts of the gluteus maximus muscles (arrows). In the thighs (C-E) there is an unusual gradient with proximal parts (C) being more replaced than distal parts (E) of the individual muscles. The vastus muscles: lateralis, intermedius and medialis (arrowheads), sartorius, gracilis and semitendinosus (stars) are more severely involved, whereas the adductor longus (circle) is relatively spared (C-E). All distal parts of the thighs only show mild fatty infiltration (E). In the lower legs (F) the anterior and lateral compartment muscles (short arrows) are severely affected. The posterior calf muscles are relatively spared.

Figure 3

Muscle biopsy sections of the vastus lateralis muscle from patient B II:1.

(A and B) Groups of fibres show marked structural alterations with splitting and numerous red or purple inclusions/deposits in trichrome stained sections (arrows).

(C) The deposits are partly eosinophilic and there are numerous internalized nuclei (Hematoxylin-eosin).

(D) NADH-terazolium reductase stained sections show pronounced structural alterations,

including rubbed out areas in some fibres (arrow).

Figure 4

Serial sections of muscle biopsy from patient B II:1 demonstrating that the purple or red deposits in trichrome staining contain actin. (A) Trichrome (B) Phalloidin-rhodamine fluorescence.

Figure 5

Immunohistochemical analysis.

(A) N-CAM is expressed in the majority of muscle fibres (Patient A III:16).

(B) Titin appears to be accumulated in some regions of abnormal fibres (Patient A IV:4).

Figure 6

Electron micrographs.

(A) In the periphery of the fibre there is an elongated deposit of dense and partly fibrillar material (arrow) with connection with altered z-disks. There is also Z-disk streaming (Patient A III:14).

(B) Irregular electron-dense inclusions with partly fibrillar structure (Patient A III:14).

Figure 7

Electron micrographs.

(A) A degenerated nucleus (arrow-head) and globular deposit of dense material surrounded by fibrillar material (arrow). There are also thickened Z-disks and occasional rod-like structures are seen (Patient B II:1).

(B) Extensive dispersion of semi-dense Z-disk derived material into and covering the entire sarcomere (Patient A III:16).

Figure 8

The identified *TTN* variant that was associated with the disease in the families.

(A) Partial sequence of *TTN* in an affected individual (left) and a healthy control (right). Red squares indicate the base position of the g.274375 T>C (AJ277892.2), p.Cys30071Arg (Q8WZ42).

(B) The substituted amino acid residue (red box) is highly conserved across vertebrate species (UCSC genome browser).

Figure 9

Mapping of a common disease haplotype in the three families A, B and C. Genome wide analysis of eight affected individuals from the families were analyzed using the RFI model (region free of incompatibilities; detailed in the materials and method section) model. 260,000 SNP loci were grouped into 2600 groups of 100 consecutive loci. Regions with 100 consecutive loci that show three or more incompatibles are shown as a black box in the chromosome plot. No incompatibilities in the group of 100 loci is indicated by one horizontal yellow box in the chromosome plot, while one to two incompatibilities (i.e. allowing for one or two genotype error in the set of in the group of 100 consecutive loci) are depicted in light grey. Note that a region on chromosome region 2q showed a strong indication of a haplotype shared by all affected members of all three families, thus indicating a common ancestral founder disease haplotype and mutation.

Figure 10

Detailed mapping of the implicated disease region on chromosome 2 using the regions free of incompatibilities model. SNP markers (n=22200) for chromosome 2 were used and in this figure they are grouped in 222 groups of 100 consecutive markers. The groups flanking the region of a low number of incompatibilities are indicated. The region extends over 769 SNP markers and 6,99 Mb of DNA on chromosome region 2q, from SNP marker rs6708551 in

position 177,367,950 to marker rs2196690 in position 184,353,132. Thus, the haplotype contains the *TTN* g.274375,T>C mutation (with genomic location chromosome 2:179,410,829) that is shared by all affected individuals. All positions are relative to the Feb.2009 – GRCh37/hg19 genome assembly.

Table 1.
Summary of clinical characteristics

Table 2.
Lung function in family A

Table 3.
Summary of muscle biopsy findings

Table 4.
Summary of statistics for exome sequencing in four individuals from family A

Table 5.
Genetic variants identified by exome sequencing of four individuals of family

References

Bang ML, Centner T, Fornoff F, Geach AJ, Gotthardt M, McNabb M, et al. The complete gene sequence of titin, expression of an unusual approximately 700-kDa titin isoform, and its interaction with obscurin identify a novel Z-line to I-band linking system. Circ Res 2001; 89:1065-72.

Birchall D, von der Hagen M, Bates D, Bushby KM, Chinnery PF. Subclinical semitendinosus and obturator externus involvement defines an autosomal dominant myopathy with early respiratory failure. Neuromuscul Disord 2005; 15:595-600.

Bucher RM, Svergun DI, Muhle-Goll C, Mayans O. The structure of the FnIII Tandem A77-A78 points to a periodically conserved architecture in the myosin-binding region of titin. J Mol Biol 2010; 401:843-53.

Caren H, Erichsen J, Olsson L, Enerback C, Sjoberg RM, Abrahamsson J, et al. High-resolution array copy number analyses for detection of deletion, gain, amplification and copy-neutral LOH in primary neuroblastoma tumors: four cases of homozygous deletions of the CDKN2A gene. BMC Genomics 2008; 9:353.

Carmignac V, Salih MA, Quijano-Roy S, Marchand S, Al Rayess MM, Mukhtar MM, et al. C-terminal titin deletions cause a novel early-onset myopathy with fatal cardiomyopathy. Ann Neurol 2007; 61:340-51.

Chapon F, Viader F, Fardeau M, Tome F, Daluzeau N, Berthelin C, et al. Familial myopathy with "cytoplasmic body" (or "spheroid") type inclusions, disclosed by respiratory insufficiency. Rev Neurol (Paris) 1989; 145:460-5.

Chinnery PF, Johnson MA, Walls TJ, Gibson GJ, Fawcett PR, Jamieson S, et al. A novel autosomal dominant distal myopathy with early respiratory failure: clinico-pathologic characteristics and exclusion of linkage to candidate genetic loci. Ann Neurol 2001; 49:443-52.

DePristo MA, Banks E, Poplin R, Garimella KV, Maguire JR, Hartl C, et al. A framework for variation discovery and genotyping using next-generation DNA sequencing data. Nat Genet 2011; 43:491-8.

Edström L, Thornell LE, Albo J, Landin S, Samuelsson M. Myopathy with respiratory failure and typical myofibrillar lesions. J Neurol Sci 1990; 96:211-28.

Jerusalem F, Ludin H, Bischoff A, Hartmann G. Cytoplasmic body neuromyopathy presenting as respiratory failure and weight loss. J Neurol Sci 1979; 41:1-9.

Krüger M, Linke WA. The Giant Protein Titin: A Regulatory Node that Integrates Myocyte Signaling Pathways. J Biol Chem 2011.

Labeit S, Kolmerer B. Titins: giant proteins in charge of muscle ultrastructure and elasticity. Science 1995; 270:293-6.

Lange S, Xiang F, Yakovenko A, Vihola A, Hackman P, Rostkova E, et al. The kinase domain of titin controls muscle gene expression and protein turnover. Science 2005; 308:1599-603.

Li H, Durbin R. Fast and accurate short read alignment with Burrows-Wheeler transform. Bioinformatics 2009; 25:1754-60.

Nicolao P, Xiang F, Gunnarsson LG, Giometto B, Edstrom L, Anvret M, et al. Autosomal dominant myopathy with proximal weakness and early respiratory muscle involvement maps to chromosome 2q. Am J Hum Genet 1999; 64:788-92.

Patel H, Berry K, MacLeod P, Dunn HG. Cytoplasmic body myopathy. Report on a family and review of the literature. J Neurol Sci 1983; 60:281-92.

Selcen D. Myofibrillar myopathies. Neuromuscul Disord 2011; 21:161-71.

Tasca G, Mirabella M, Broccolini A, Monforte M, Sabatelli M, Biscione GL, et al. An Italian case of hereditary myopathy with early respiratory failure (HMERF) not associated with the titin kinase domain R279W mutation. Neuromuscul Disord 2010; 20:730-4.

Udd B, Partanen J, Halonen P, Falck B, Hakamies L, Heikkila H, et al. Tibial muscular dystrophy - late Adult-Onset distal myopathy in 66 finnish patients. Arch Neurol 1993; 50:604-8.

Udd B, Vihola A, Sarparanta J, Richard I, Hackman P. Titinopathies and extension of the M-line mutation phenotype beyond distal myopathy and LGMD2J. Neurology 2005; 64:636-42.

Winter JH, Neilly JB, Henderson AF, Stevenson RD, Doyle D, Wiles CM, et al. Life-threatening respiratory failure due to a previously undescribed myopathy. Q J Med 1986; 61:1171-8.

Xiang F, Nicolao P, Chapon F, Edstrom L, Anvret M, Zhang Z. A second locus for autosomal dominant myopathy with proximal muscle weakness and early respiratory muscle involvement: a likely chromosomal locus on 2q21. Neuromuscul Disord 1999; 9:308-12.

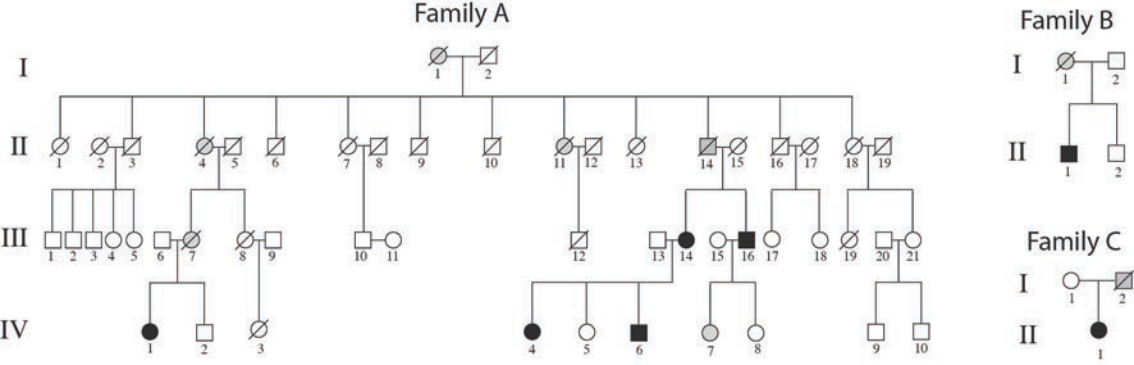
Family A
I
II
III
IV
Family B
I
II
Family C
I
II

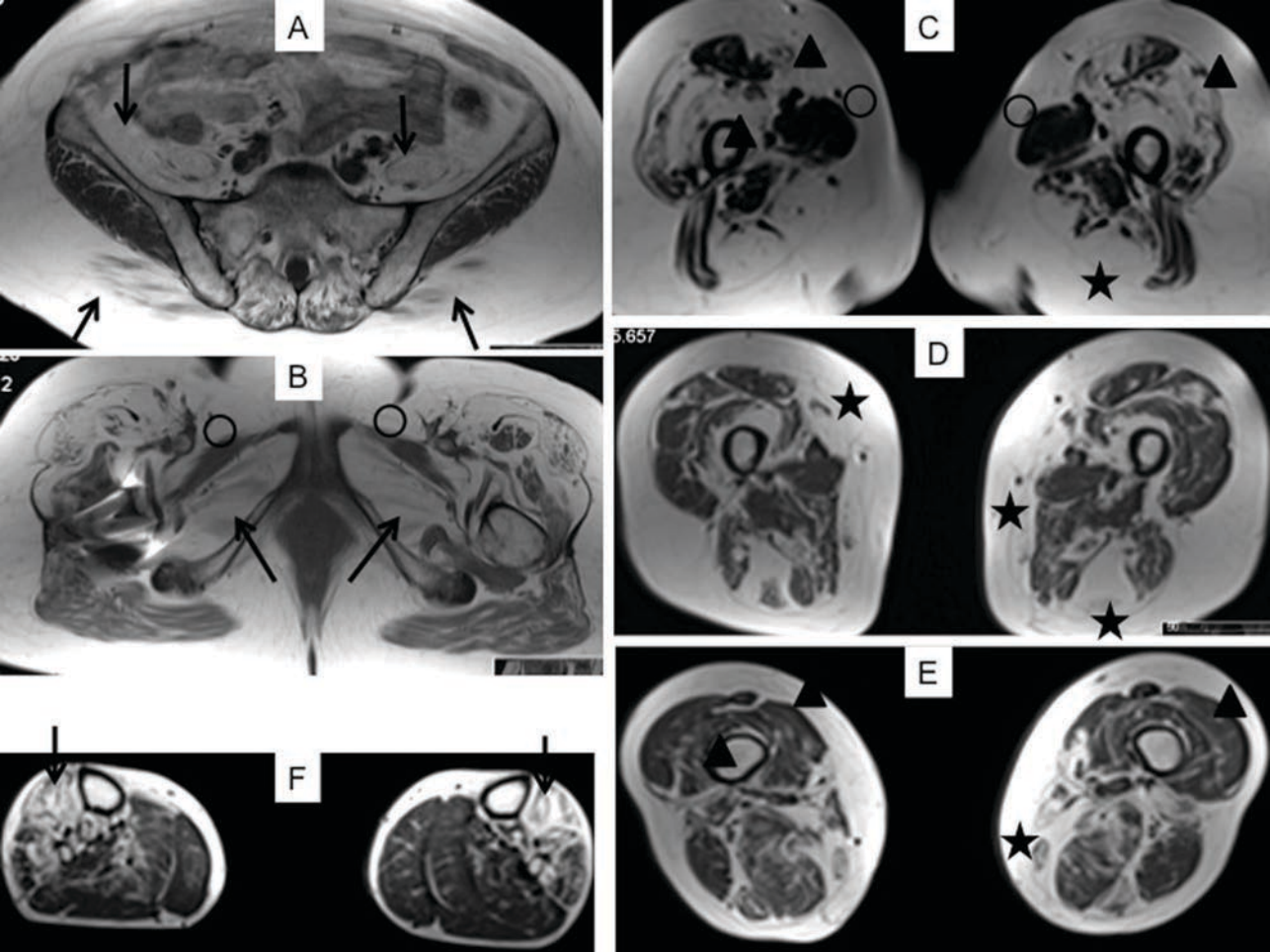
A
B
C
D
E
F

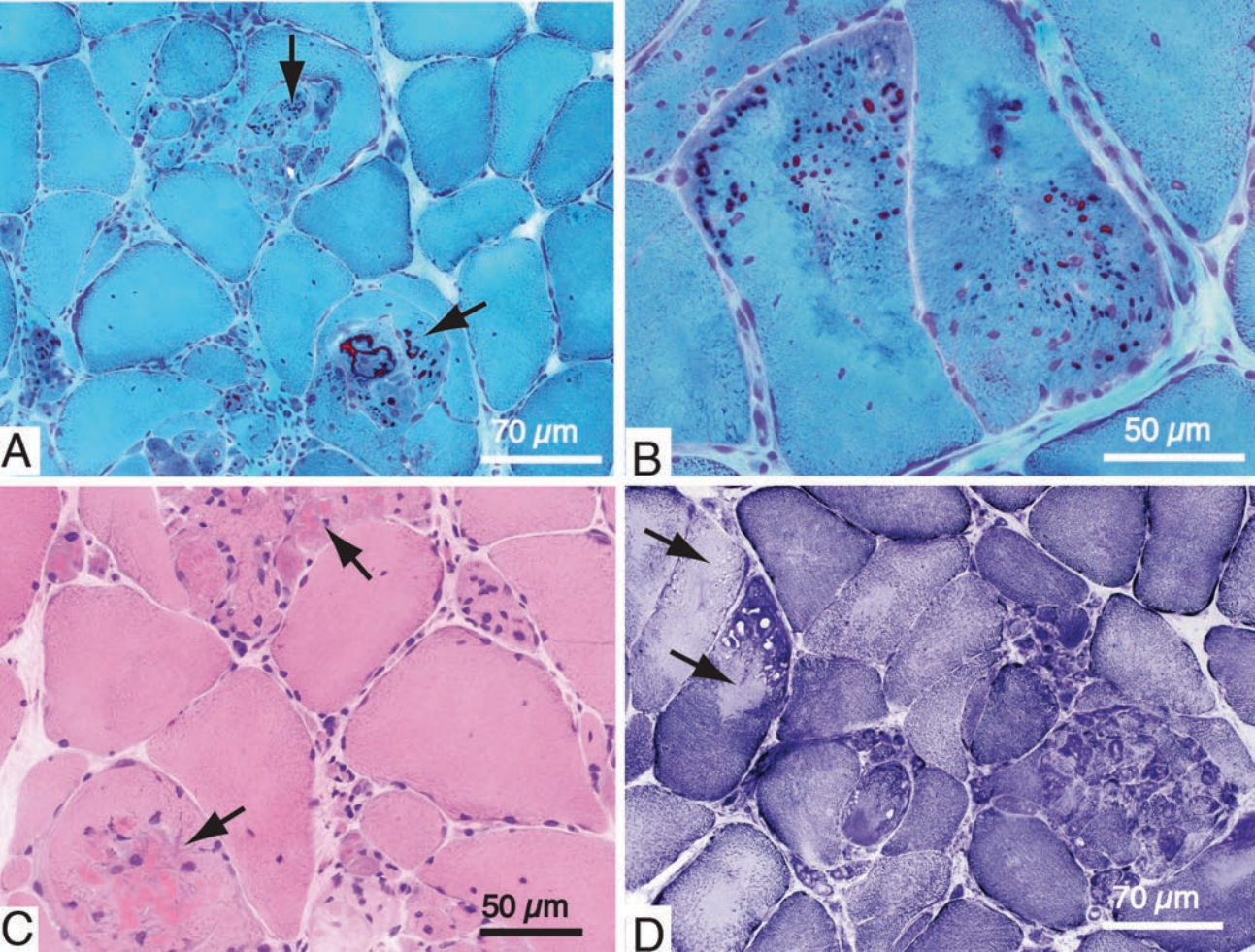
A
70 μm
B
50 μm
C
50 μm
D
70 μm

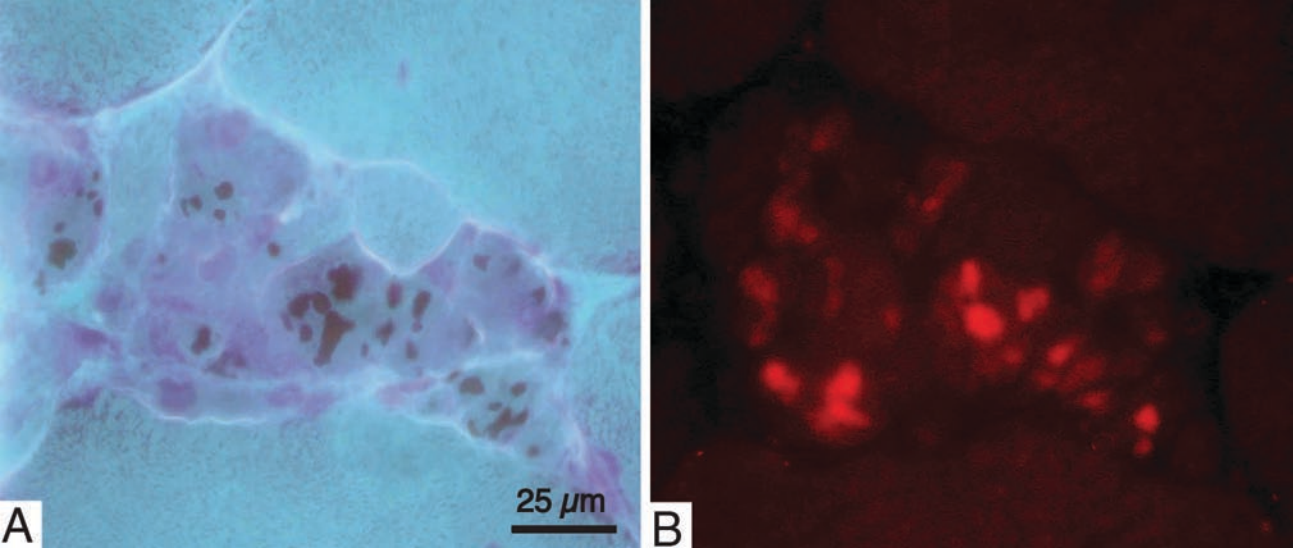
25 μm
A
B

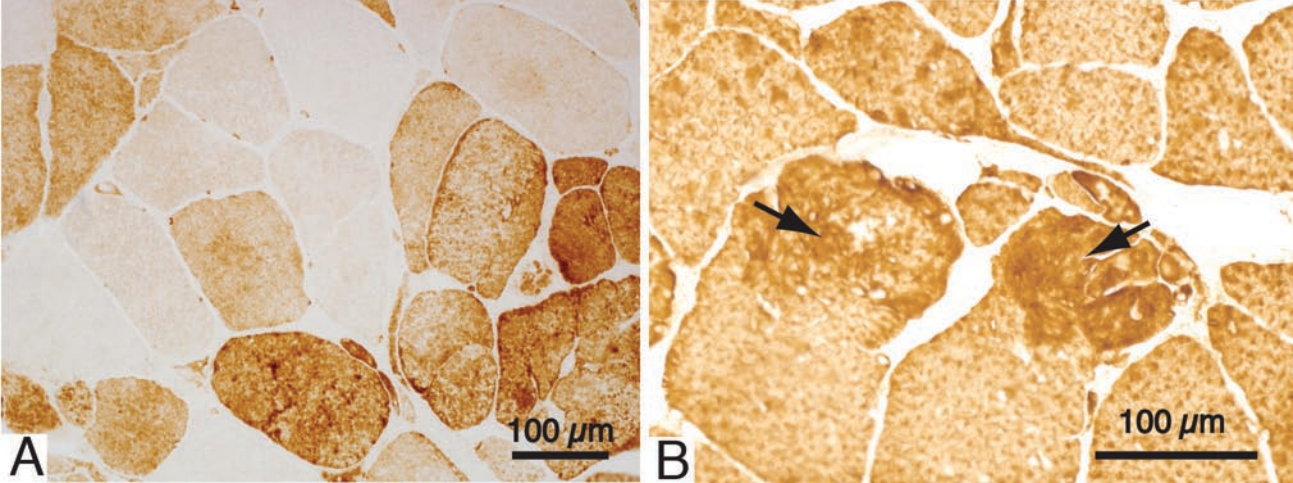
A
100 μm
B
100 μm

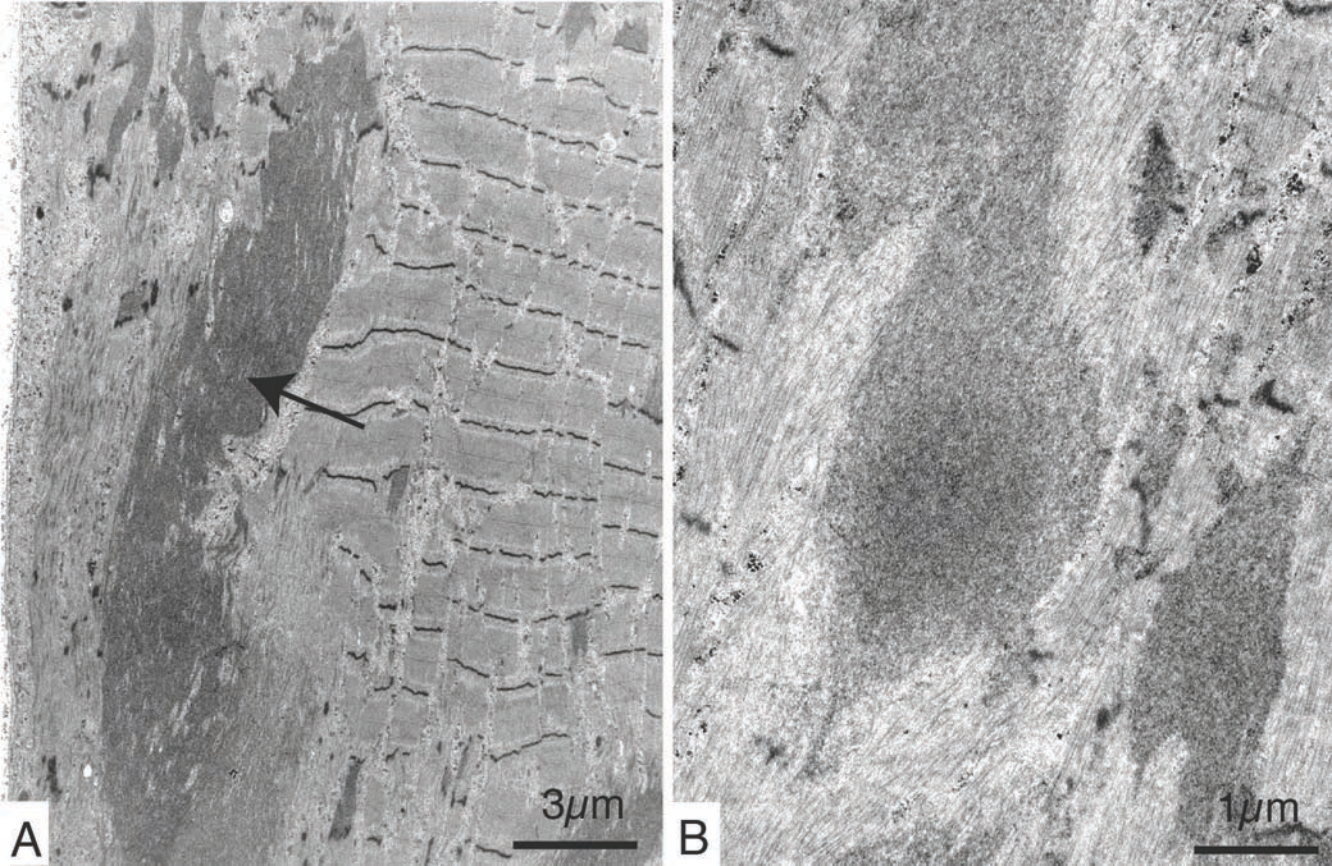
A
3μm
B
1μm

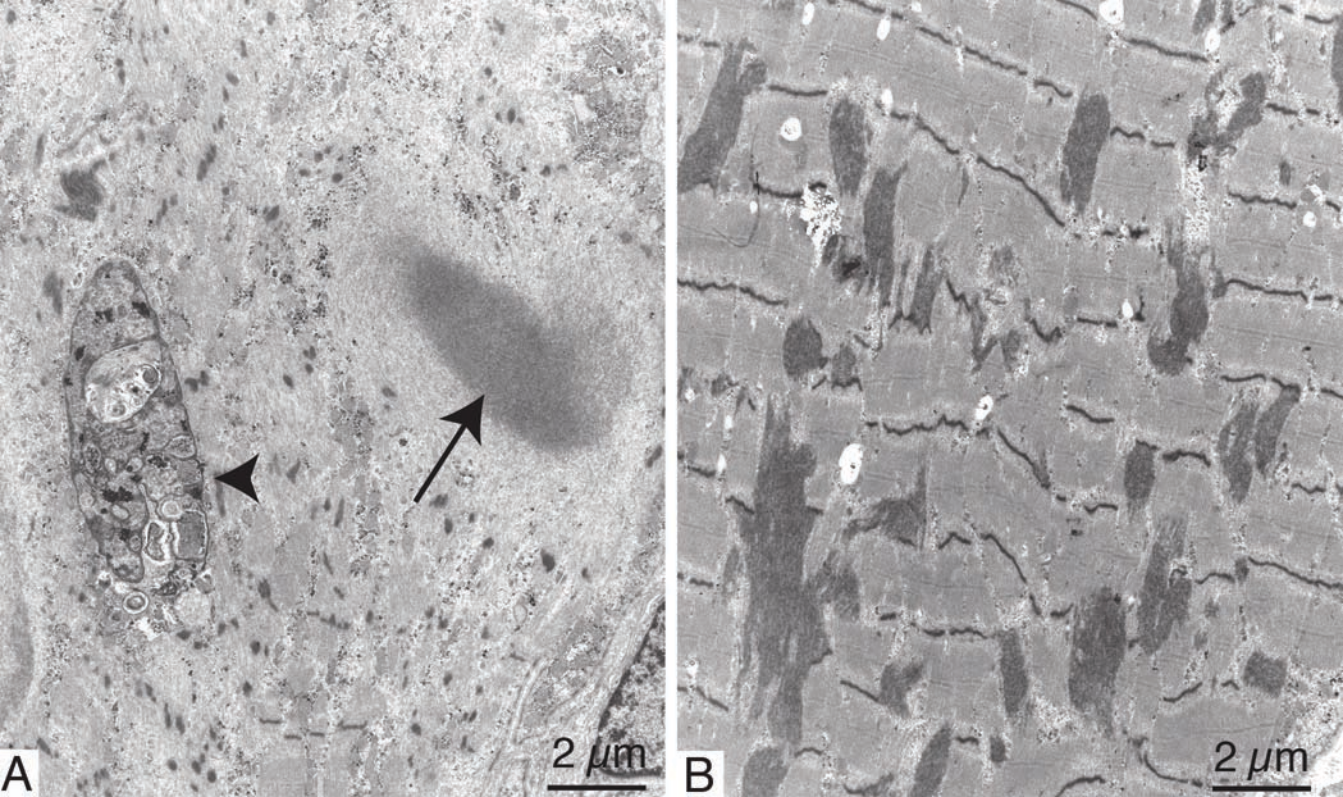
A
2 μm
B
2 μm

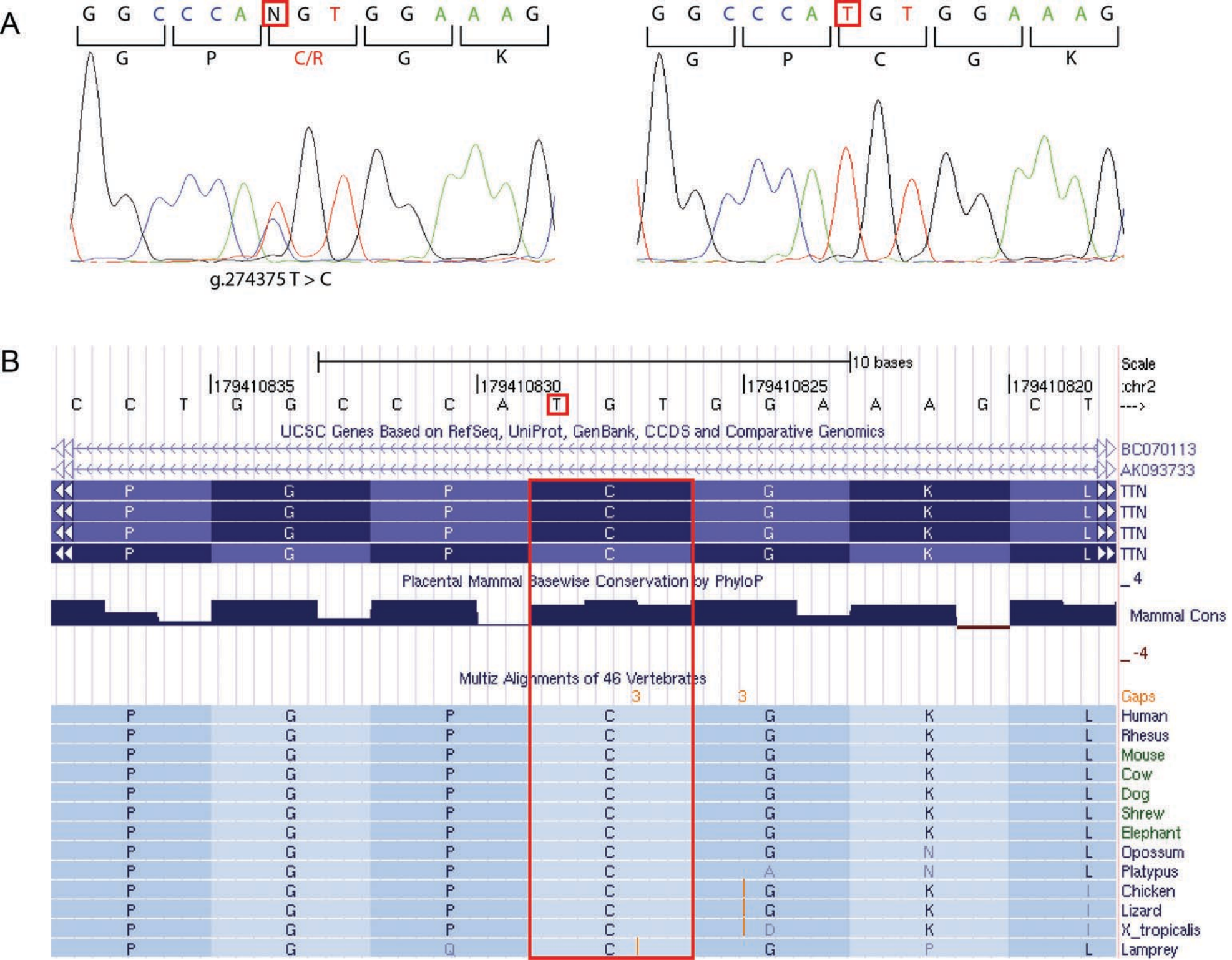
A
G G C C C A N G T G G A A A G
G P C/R G K
g.274375 T > C
G G C C C A T G T G G A A A G
G P C G K
B
10 bases
179410835
179410830
179410825
179410820
Scale
chr2
C C T G G C C C A T G T G G A A A G C T
UCSC Genes Based on RefSeq, UniProt, GenBank, CCDS and Comparative Genomics
BC070113
AK093733
P G P C G K L TTN
P G P C G K L TTN
P G P C G K L TTN
P G P C G K L TTN
Placental Mammal Basewise Conservation by PhyloP
4
Mammal Cons
-4
Multiz Alignments of 46 Vertebrates
Gaps
P G P C G K L Human
P G P C G K L Rhesus
P G P C G K L Mouse
P G P C G K L Cow
P G P C G K L Dog
P G P C G K L Shrew
P G P C G K L Elephant
P G P C G N L Opossum
P G P C A N L Platypus
P G P C G K I Chicken
P G P C G K I Lizard
P G P C D K I X_tropicalis
P G Q C G P L Lamprey


1
2
3
4
5
6
7
8
9
10
11
12
13
14
15
16
17
18
19
20
21
22
X

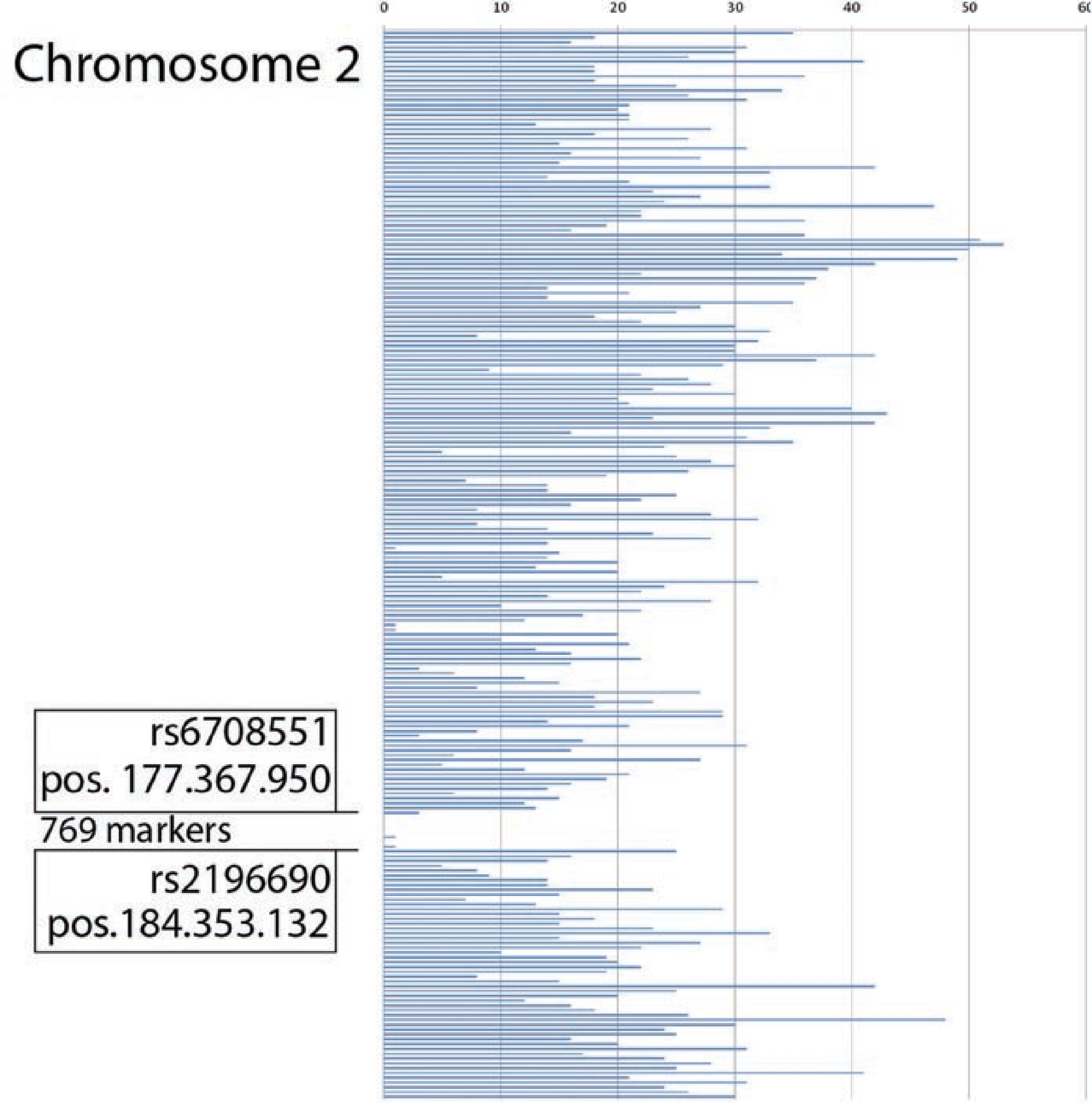
Chromosome 2
0
10
20
30
40
50
rs6708551
pos. 177.367.950
769 markers
rs2196690
pos.184.353.132

Table 1. Summary of clinical characteristics

Patient (sex)	**AIII:14 (F)**	**AIII:16 (M)**	**AIV:1 (F)**	**AIV:4 (F)**	**AIV:6 (M)**	**AIV:7 (F)**	**BII:1 (M)**	**CII:1 (F)**
Age at onset (years)	30	35	30	40	20	18	22	36
Initial symptoms	Weakness in shoulder girdle	Weakness in ankle dorsi-flexors	Myalgia and weakness in pelvic gidle	Weakness in shoulder and pelvic girdle	Myalgia	Weakness in pelvic girdle	Weakness in ankle dorsi-flexors	Respiratory insufficiency
Age at initial symptoms of respiratory insufficiency	55	40	35	Asymptomatic	20	20	30	36
Age at investi-gation (years)	67	66	56	49	41	37	43	45
Facial muscles	Mild weakness in m. frontalis	Normal	Normal	Mild weakness in m. frontalis	Mild weakness in m. frontalis	Mild weakness in m. frontalis	Normal	Normal
Neckflexor muscles	2	3	1	2	4	1	2	2
Trunk muscles	1	2	1	1	2	1	1	2
Shoulder flexion and abduction	4	5	5	1	5	4	2	nd
Elbow flexion	5	5	5	5	5	5	4	nd
Elbow extension	5	5	5	4	5	4	4	nd
Wrist flexion	5	5	5	5	5	5	3	5
Wrist extension	5	5	5	5	5	5	3	5
Finger flexion	5	5	5	5	5	5	2	5
Finger extension	5	5	5	5	5	5	3	5
Hip flexion	2	4	3	1	2	1	1	2
Hip abduction	3	4	4	1	3/4	2	1	3
Knee flexion	3	5	3	2	3	1	1	2
Knee extension	5	5	5	5	5	5	4	3
Ankle dorsiflexors	3	1	5	1	1	1	1	2
Ankle extensors	5	5	5	5	5	5	3	5
Calf hypertrophy	Yes	Yes	Yes	Yes	Yes	Yes	Yes	nd

Muscle strength graded (0-5) according to Medical Research Council scale (MRC). The muscle strength were symmetrically distributed and MRC grades refer to both left and right side except in hip abduction in patient AIV:6. nd = not determined

Table 2. Lung function in family A

Patient (sex)	**Age (yr)**	**Respiratory symptoms**	**VC standing (L)**	**VC in % of predicted normal**	**VC supine (L)**	**PCO2 at day-time (normal 4.4-6 kPa)**
AIII:14 (F)	67	Shortness of breath during exercise from age 55 y	1,2	50	1,1	5,18
AIII:16 (M)	66	Shortness of breath during exercise from age 40 y, nocturnal NIV from age 55 y	1,05	30	0,75	6,2
AIV:1 (F)	56	Asthma, shortness of breath during exercise from age 35 y	2	74	1,92	ND
AIV:4 (F)	49	Asymptomatic	1,8	58	1,76	4,9
AIV:6 (M)	41	Shortness of breath during exercise from age 20 y, nocturnal NIV from age 35 y	2,2	54	1,6	6,4
AIV:7 (F)	37	Shortness of breath during exercise from age 20 y, nocturnal NIV from age 37 y	0,73	20	0,54	9,7

VC = vital capacity, L = litres, ND = not determined, NIV = noninvasive ventilation.

Table 3. Summary of muscle biopsy findings

Patient	**AIII:14**	**AIII:16**	**AIV:1**	**AIV:4**	**AIV:6**	**BII:1**	**CII:1**
Age at biopsy	56/66	58/58/65	43	41/48	33/40	29	44
Muscle	TA/QVL	TA/D/QVL	TA	TA/TA	TA/TA	TA	QVL
Type 1 fibers (%)	40/50	60/40/30	80	90/90	80/80	60	70
Fat and fibrous tissue replacement	-	-	almost total	marked/ almost total	-/ almost total	-	-
Internal nuclei	+/+	+++/+++/-	+	+++/+++	+++/+++	+++	++
Fiber splitting	+/+	++/+/-	+	+/+	+/++	+	+
Rimmed vacuoles	+/-	+/+/-	+	++/-	++/++	++	++
Eosinophilic inclusions/ cytoplasmic bodies	+/++	+/++/+	+	+/++	++/+	++	++
Nectrotic fibers	-/-	-/-/-	-	-/-	-/++	-	+
Interstitial inflammatory cells	-/-	+/-/-	-	-/-	-/-	-	-
Fibers with large, unstained regions in NADH-TR staining	-/+	+/+/-	+	+/-	++/-	+	+

TA= tibialis anterior, QVL= quadriceps vastus lateralis, D= deltoideus, - = not found, + = found but not abundant, ++ = abundant, +++ = in majority of muscle fibers.

Table 4. Summary of statistics for exome sequencing in four individuals from family A

Sample	Total reads	Genome	%	Duplicates	%	Target	%
IV:2	50,133,338	49,776,532	99.3%	1,502,228	3.0%	31,675,785	63.6%
IV:5	42,541,494	42,237,601	99.3%	948,740	2.3%	27,198,270	64.4%
III:14	40,517,614	40,230,724	99.3%	1,288,363	3.2%	25,870,566	64.3%
III:16	40,579,248	40,289,842	99.3%	1,442,547	3.6%	26,261,503	65.2%

Total reads: total reads in the sample
Genome: reads placed on the genome
Duplicates: reads that could be due to PCR amplification marked by the software. They are not considered for further analysis
Target: reads mapped to exon regions defined by the Agilent's SureSelect Enrichment baits

Table 5. Genetic variants identified by exome sequencing of four individuals of family A

Filter	**A IV:2 Healthy**	**A IV:5 Healthy**	**A III:14 Affected**	**A III:16 Affected**	**Variants only in the two affected individuals**
Indels not in dbSNP131	1101	988	954	958	71
Novel indels in CDS and SS	458	405	368	400	21
SNPs not in dbSNP131	3940	3519	3637	3580	373
Novel non synonymous SNPs and SS variants	2050	1990	2022	1986	147

SS = splice site, CDS = Coding sequence